Magnetoencephalography in the Study of Cortical Auditory Processing

Minna Huotilainen

Thesis for the degree of Doctor of Technology

Teknillinen korkeakoulu
Sähkö- ja tietoliikennetekniikan osasto
Akustiikan ja äänenkäsittelytekniikan laboratorio

Helsinki University of Technology
Department of Electrical Engineering and Communications
Laboratory of Acoustics and Audio Signal Processing

Otaniemi 1997/Raportti 43

Helsinki University of Technology
Department of Electrical and Communications Engineering
Laboratory of Acoustics and Audio Signal Processing

Magnetoencephalography in the Study of Cortical Auditory Processing

Minna Huotilainen

Thesis for the degree of Doctor of Technology

Report 43

ISBN 951-22-3435-1
ISSN 0356-083X

HELSINKI UNIVERSITY OF TECHNOLOGY
FACULTY OF ELECTRICAL ENGINEERING
LABORATORY OF ACOUSTICS AND AUDIO SIGNAL PROCESSING

Magnetoencephalography in the study of cortical auditory processing

Minna Huotilainen
COGNITIVE BRAIN RESEARCH UNIT
DEPARTMENT OF PSYCHOLOGY
UNIVERSITY OF HELSINKI

Dissertation for the degree of Doctor of Technology to be presented with due permission for public examination and debate in the Auditorium XII of University of Helsinki on the 7th of February, 1997, at 12 noon.

Helsinki 1997

Magnetoencephalography in the study of cortical auditory processing

Minna Huotilainen

Abstract

This thesis deals with the auditory system of the human brain. Seven publications presenting magnetoencephalographic (MEG) results on the functional organization of the auditory cortex and source modelling of MEG data are presented. The data, displaying brain structures which are organized according to stimulus features and related to the detection and short-term memory responses of the auditory system, were mostly gathered using the Neuromag-122 whole-head magnetometer. New methods to whole-head MEG data analysis were reported in order to utilize the data obtained with the magnetometer.

The experimental paradigms in the publications of this thesis dealt with the tonotopic and ampliotopic organization of the auditory cortex, the processing of simple and complex sounds, and auditory memory. The data was analyzed using dipole models, minimum-norm estimation and signal-space projection method.

Keywords: auditory system, magnetoencephalography, tonotopy, ampliotopy, N1m, mismatch negativity, equivalent current dipole, minimum-norm estimate, signal space projection method

Acknowledgements

The studies included in this thesis were carried out in the Cognitive Brain Research Unit (CBRU, Department of Psychology, University of Helsinki), which has been selected as one of the *Centers of Excellence* in Finland several times. Having now worked for five years in this unit, I owe my greatest gratitude to the whole group. First, I want to thank Academy Professor Risto Näätänen for guiding my work in a manner that has been warm and supportive and, on occasion, taught me to carry responsibility.

My warmest thanks belong to my supervisor Risto Ilmoniemi, who taught me to work hard and apply high standards to all aspects of my work. His personality and attitude towards science has been a true delight and the driving force of my work. I want to acknowledge the flexibility of Professor Matti Karjalainen and the support he gave me in the preparation of this multidisciplinary thesis.

I wish to thank my close collaborators Kimmo Alho for his never-ending energy, optimism, and his vigorous knowledge of his field of expertise and Hannu Tiitinen for his time, interest, encouragement, and openminded attitude towards science and life in general. I also wish to thank Janne Sinkkonen, Teija Kujala, and Juha Lavikainen for devoting time to our close and fruitful scientific collaboration.

I want to thank the personnel of CBRU, especially Katina Buch Lund, Marie Cheour-Luhtanen, Iiro Jääskeläinen, Sirkka-Liisa Joutsiniemi, Anne Lehtokoski, Petri Paavilainen, Patrick May, Eero Pekkonen, Kalevi Reinikainen, Teemu Rinne, Wolfgang Teder, Mari Tervaniemi, Juha Virtanen, and Istvan Winkler.

I want to thank Antti Ahonen and his crew at Neuromag, Matti Hämäläinen, Matti Kajola, Jukka Knuutila, Petteri Laine, Lauri Parkkonen, and Juha Simola, for doing more than their share for the advancement of my thesis.

I express my gratitude to Professor Olli V. Lounasmaa and his very exceptional personnel at Low Temperature Laboratory (Helsinki University of Technology) for giving me the opportunity to use their magnetometer. During my stay at Low Temperature Laboratory I was priviledged to follow the marvellous management strategy of Professor Lounasmaa utilizing the best qualities of each researcher.

Several of the experiments included in this thesis were performed in the BioMag Laboratory (Helsinki University Central Hospital). I want to thank all people working there for creating an incredibly pleasant working atmosphere. Special thanks are due to Antti Korvenoja, Kirsi Lauerma, Sami Martinkauppi, Matias Palva, Teemu Peltonen, Jarmo Ruohonen, Leena Sipilä, and Heidi Wikström.

Jari Karhu and Professor Claudia Tesche deserve thanks for supporting me and my work. I wish to thank Suvi Heikkilä, Marja Holmström, and Maritta Maltio-Laine for their help in practical matters. I want to thank the Department of Radiology, Helsinki University Central Hospital, for providing me with the magnetic resonance images needed in this study. I want to thank Professor Toivo Katila and Professor Unto K. Laine for their interest in my work. I thank my scientific examinors Professor Yoshio Okada and Jukka Nenonen for good and profound comments on the thesis.

I wish to thank all my friends for supporting me. I am ever grateful to my parents Marja-Leena and Lars Colérus and my brother Harri Colérus, for they never stopped believing in me. I want to thank my husband Tommi for always being there for me.

1 Introduction

The rapidly developing field of cognitive neuroscience combines multiple disciplines such as mathematics, physics, psychology, biology, chemistry, and medicine. The technology needed to explore brain activity is developing rapidly. Mathematical models are being introduced to interpret the data, new experimental paradigms to clarify the brain processes in different tasks are being applied, and theories of brain function are becoming more and more specific.

The data of five of the seven publications included in this thesis were gathered using the Neuromag-122 whole-head magnetometer [3]. The construction of this instrument was completed in 1992 representing the most recent advancement in the measurement of magnetic fields and making Finland the leading country of magnetoencephalography (MEG) instrumentation. The device covers the head with 122 sensors, thus allowing whole-head MEG measurements with only one positioning of the instrument. To develop methods for data analysis, the goal of this thesis, is necessary in order to fully utilize the data obtained with this device.

The experimental paradigms in the publications of this thesis dealt with the tonotopic and ampliotopic organization of the auditory cortex and the processing of simple and complex sounds. The data was analyzed using dipole models, minimum-norm estimation and signal-space projection method. In Publication I, the stimulus-change detection system that is reflected by the mismatch response (MMNm) for complex sound patterns was found to be located in or near the auditory cortex. In Publication II, the source of the MMNm was found to be tonotopically organized. In Publication III, plasticity in the adult human brain was studied by using the minimum-norm estimate (MNE) projected onto the surface of the brain – a new way for MEG data presentation. In Publication IV, on the basis of the amplitude changes of the MMNm it was suggested that, for a given stimulus frequency, there exists processing capacity which is separable from processing of other stimulus features.

In Publication V, a new data-analysis method, the signal-space projection (SSP), was introduced and its applicability in rejecting or suppressing blink artefacts from auditory evoked response data was demonstrated.

In Publication VI, the evoked sustained response to tones, the sustained field (SF), was found to have its source in a tonotopically organized cortical area, whose tonotopy resembles that of another, transient evoked response, the N1m. In Publication VII, evidence for ampliotopy in the auditory area producing the N1m response was found by estimating source locations for responses to tones of different amplitudes and by applying a model of refractoriness to

the source strengths.

In Section 2, after a brief presentation of the basic principles of acoustics and the functioning of the ear, the anatomy of the auditory pathways, and the organization of the auditory cortex are reviewed in more detail. The event-related responses of the brain are briefly reviewed in Section 3.

Methodology for studying brain activity along with some applications is presented in Section 4, with the emphasis on three MEG data analysis methods, the dipole model (ECD), the minimum-norm estimate (MNE), and the projection method (SSP). In Section 5, the three analysis methods are applied to a set of data where multiple sources are simultaneously active, and their relative merits are discussed.

Thereafter, general conclusions are presented on the applicability of the different analysis methods in analysing MEG data. Finally, the *List of Publications* is presented and each publication is summarized.

2 From vibrations of the air to electric activity patterns in the brain

2.1 Vibrations of the air — acoustics

Sound, a wave of increases and decreases of air pressure, can result from mechanical movement of, for example, a string of a guitar. The frequency of the sound (subjectively perceived as pitch) is expressed as the number of cycles per second, i.e., in Hertz (Hz).

The sound amplitude (perceived as loudness) is the magnitude of change in the air pressure, typically expressed in the decibel scale: $A=20\log_{10}(P/P_0)$, where $P_0=20\ \mu\mathrm{N/m}^2$. The reference pressure P_0 is required to make a sound of 1 kHz just audible to the average healthy listener, and corresponds to 0 dB. The human ear is able to respond to frequencies from 20 Hz to 20 kHz and, without pain, to a 120-dB range of sound pressures.

The location of a sound source is estimated by comparing the signals arriving in the two ears. When the distances from the sound source to the ears are different, the two signals differ in amplitude, onset time, phase, and frequency spectrum. At frequencies below 1.5 kHz, the interaural time difference is used as a cue for estimating the location of the sound source, whereas interaural intensity difference is used at frequencies higher than 1 kHz.

2.2 The human ear

The human ear [78] consists of the outer, the middle, and the inner ear (see Fig. 1A). The outer ear guides the sound waves to the tympanic membrane, affects sound perception by amplifying frequencies at about 1 and at about 4 kHz [98], and makes sound source location estimation easier by adding echoes which depend on the angle between the pinna and the incoming sound.

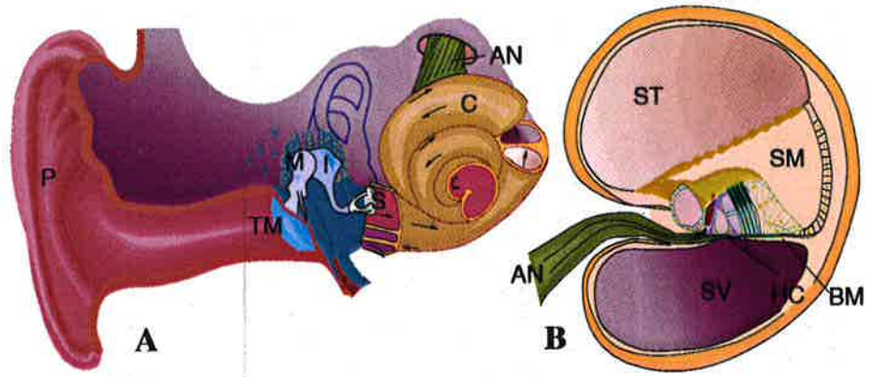

Figure 1: **A)** The pinna (P) reflects the sound waves to the tympanic membrane (TM). The oscillation moves the bones of the middle ear, malleus, incus, and stapes (M, I, S), which relay the sound to the cochlea (C) of the inner ear. **B)** The three compartments of cochlea, the scala tympani (ST), the scala vestibuli (SV), and the scala media (SM), and the basilar membrane (BM) oscillate and move the stereocilia of the hair cells (HC), which in turn send electric pulses to the auditory nerve (AN).

The middle ear is an impedance transducer: it transmits the vibration from the air to the fluid-filled inner ear. Without the middle ear, the vibration would meet a high acoustic impedance barrier and most of its energy would thus be reflected.

The most important contributors to the impedance matching are the *ossicles*, the three small middle-ear bones (malleus, incus, and stapes). The stapes is attached to the oval window, a small opening in the cochlea, and mediates the vibration into the inner ear.

The cochlea (Fig. 1B), a spiral bone cavity, consists of three liquid-filled compartments [98], all of which oscillate in step with the stapes. The *organ of Corti* rests on the basilar membrane. The mechanical movement is transformed into electric pulse patterns in the *hair cells* situated in the organ of Corti. The hair cells are arranged into three to five rows of outer and one row of inner hair cells.

On the apical surface of each hair cell there is a bundle of *stereocilia* containing actin, which has been proposed to be a key factor in the active change of stiffness of the stereocilia [79]. The bundles are displaced when the tectorial and basilar membranes move with respect to each other. The displacement opens ion channels mechanic-

ally [8, 14], current flows into the hair cell, and the cell is depolarized.

Connected to each outer hair cell, there are two to six terminals of afferent nerve fibers [62], each synapsing with only one hair cell. There are also efferent endings synapsing on the afferent terminals and directly on the outer hair cell. Connected to each inner hair cell, there are six to eight afferent nerve fibers [63], each fiber synapsing with several inner hair cells. There are also efferent fibers making contact with the afferent terminals.

The depolarization of the hair cell causes neurotransmitter release at the base of the cell. The transmitter excites the afferent neurons connected to the cell and initiates action potentials in the ascending neurons of the auditory nerve. Approximately half of the fibers of the auditory nerve are ascending and the rest descending [2].

In the cochlea, information on the sound signal, i.e., its amplitude, frequency spectrum, and phase relationships, is transformed into a partly *digital* representation; there is no quantization in the timing of the nerve impulses, but the quantum of the response size is one action potential. The axons of the auditory nerve have a characteristic response pattern to sound stimulation: The probability of the cells to fire is greatest at the beginning of the sound. During the sound, the probability is greatest at the rising edge of the sound signal. After the end of the sound, the firing probability drops briefly under spontaneous firing level.

When a sound enters the ear, it results in a traveling wave that progresses along the length of the cochlea, starting at the oval window [17]. The basilar membrane and the hair cells are mechanically tuned in a *tonotopical* arrangement: along the basilar membrane, the location of each cell is in an approximately logarithmic relation to the frequency it is tuned to. Thus, each octave maps onto an area which is about 3 mm long on the basilar membrane. High-frequency sounds cause a standing wave peaking at the base, near the oval window, whereas low-frequency sounds cause strongest oscillations near the apex.

At the base of the cochlea the basilar membrane is narrow and stiff, and the outer hair cells and their stereocilia are short and rigid. At the apex the basilar membrane is more flexible, and the hair cells and their stereocilia are more than twice as long as and more flexible than those at the base.

The amplitude of the sound signal affects the response pattern of the hair cells in two ways: The cells fire more actively during louder than during softer sounds. Also, a broader region of cells around the characteristic frequency fire during louder than during softer sounds.

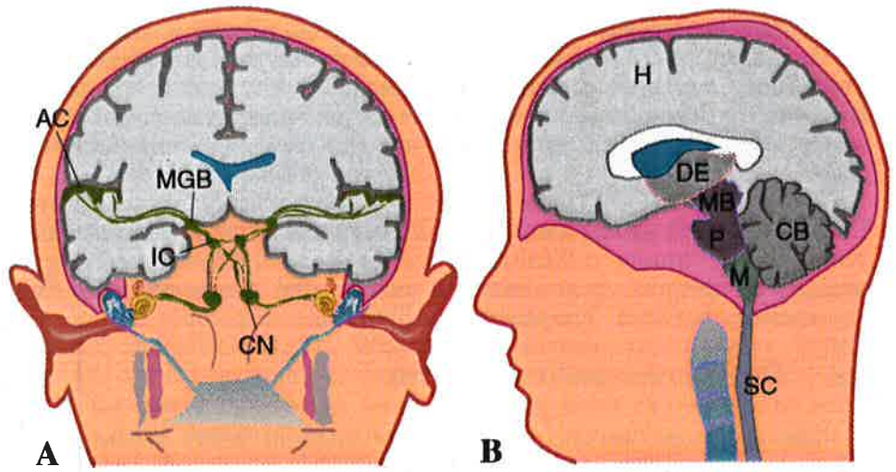

Figure 2: **A)** The auditory pathways from the ears to the auditory cortices are presented with green. After the cochlear nucleus (CN) in the ipsilateral side, the main pathway crosses to the contralateral side to the inferior colliculus (IC), medial geniculate body (MGB) of the thalamus, and the auditory cortex (AC). **B)** The human brain is seen from the left. The central nervous system consists the spinal cord (SC), the medulla (M), the pons (P), the cerebellum (CB), the midbrain (MB), the diencephalon (DE), and the cerebral hemispheres (H).

2.3 From the ear to the brain

The auditory pathways are presented in Fig. 2A. The ipsilateral *cochlear nucleus* is the first nucleus of the auditory pathway. It has three divisions, anteroventral, posteroventral, and dorsal, all of which are tonotopically organized [51]. Most of the response patterns of the cells in the cochlear nucleus are similar to those in the cochlear nerve, but sustained responses and responses to onsets and offsets of sound are also found [2]. This indicates that, in addition to the features already presented in the auditory nerve, new features of the sound, related mainly to sound duration, are derived in the cochlear nucleus [68] before feeding the patterns forward.

From the ipsilateral cochlear nucleus, the main auditory pathway projects to the contralateral *superior olivary complex* (SOC), which is the first nucleus of binaural integration, receiving input from both cochlear nuclei. The main parts of SOC are the medial SOC, sensitive to interaural time differences of low-frequency sounds, and the lateral SOC, sensitive to interaural intensity differences of high-frequency sounds. This suggests that the

SOC processes mainly the location of the stimulus [23]. Fibers from both SOCs and both cochlear nuclei enter the *nucleus of lateral lemniscus*, which in turn projects to the *inferior colliculus*.

The *medial geniculate body* (MGB) of the thalamus receives input from the inferior colliculus and projects to the primary and secondary auditory cortices. The thalamus might be a gating mechanism of information entering the cortex; it might be involved in the maintenance of consciousness (for a review on thalamocortical interaction, see Nunez [67]). In the MGB, there is a tonotopically organized ventral nucleus and two non-tonotopically organized divisions receiving also visual and somatosensory inputs [98].

2.4 The human auditory cortex

The auditory cortex in each hemisphere (see Fig. 2A) is located on the upper surface of the temporal lobe, in the Heschl's gyrus in the Sylvian fissure [77]. The human auditory cortex consists of *primary auditory cortex* (AI) surrounded by secondary auditory areas (AII) [98].

The AI and at least some of the AII areas are tonotopically organized, containing several maps of the audible frequency spectrum. These organizations have been observed in cortical recordings [12, 39], by electroencephalography (EEG) [10, 96], by MEG [19, 72, 85, 104], and by positron emission tomography (PET) [48].

In monkeys, single cells in auditory cortex display a variety of frequency tuning curves including sharp, broad, and multiple-minima tuning. The characteristic frequencies of the cells with sharp frequency-tuning curves cover the whole range of audible frequencies.

Ampliotopy of the human auditory cortex has been suggested on the basis of MEG recordings [71]. In monkeys, intensity-tuning curves with their best intensities covering the range of 15 to 95 dB have been reported [11], suggesting cortical organization according to stimulus intensity. The left and right temporal cortices are highly asymmetric [20, 99]. With respect to bony landmarks, the responses to tones are located significantly higher and tend to be more posterior over the left hemisphere [84].

This is also reflected as a functional difference between the hemispheres. Almost all right-handed people have their speech functions lateralized to the left hemisphere and perform better in verbal auditory tasks when the task is presented to the right ear [40].

The primary auditory cortex projects to several association regions. Broca's area is located in the frontal lobe usually in the left hemisphere and is involved in the production of speech. Wernicke's area is located in the temporal lobe posterior to the auditory cortex usually in the left hemisphere and it is involved in the processing of complex auditory information such as phonemes.

The left and right auditory cortices are interconnected through the corpus callosum; transfer times vary between 3 and 30 ms [52]. The connections originate typically at the homologous loci from the other hemisphere.

3 Event-related correlates of brain activation

The functioning of the human brain can be studied noninvasively using EEG and MEG [31, 34]. When nerve cells are active, small currents flow in the tissue producing weak magnetic fields measurable outside the head and changes of electric potential on the surface of the head. The transmembrane currents of a large group of synchronously activated cortical pyramidal cells are the major contributor to the surface-recorded electric potentials and magnetic fields [15, 25, 66, 46]).

Because of the almost spherical symmetry of the head, most of the MEG signal is produced by the tangential component of the cortical currents, while both radial and tangential components contribute to the EEG signal. In addition, MEG is less sensitive to currents deep in the brain than EEG. Because of these differences, a simultaneous EEG and MEG measurement can be shown to give more information than the use of the same number of EEG or MEG channels alone.

EEG and MEG differ fundamentally from metabolic brain imaging methods such as positron emission tomography (PET) and functional magnetic resonance imaging (fMRI): by measuring electric potentials and magnetic fields caused by the active neurons themselves, it is possible to study the information processing in the brain on a millisecond scale.

Event-related potentials, ERPs, and event-related magnetic fields, ERFs, are averages of continuous EEG and MEG signal time-locked to an event, for example the presentation of a stimulus. Depending on the response size and the noise level, the stimulus or task is repeated typically 50–500 times and the epochs of EEG and MEG are averaged in order to extract the ERP and ERF from the background EEG and MEG activity and noise.

Auditory event-related responses (see Fig. 3 for an example) consist of short-latency (0–10 ms), middle-latency (10–50 ms), and long-latency (50–500 ms) responses, most prominent of which are the P50(m), the N1(m), and the P2(m), * peaking on the average at 50, 100, and 200 ms after the stimulus onset, re-

*Here, P50, N1, P2, and SP are electric responses, P50m, N1m, P2m, and SF their magnetic counterparts, and P50(m), N1(m), and P2(m) refer to both electric and magnetic responses.

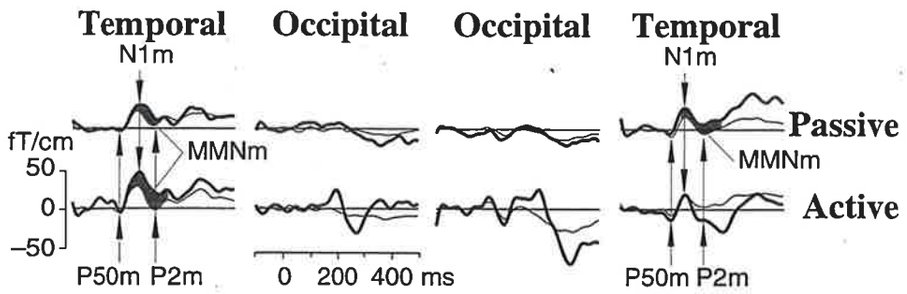

Figure 3: ERFs of SK, a blind subject from Publication III. Responses to the standard (thin line) and deviant (thick line) tones in the temporal (left and right) and occipital (middle columns) channels. In the passive condition (upper row), the subject was reading Braille and ignoring the tones. In the active condition (lower row), the subject was counting the deviant tones. The P50m, the N1m, and the P2m peaks are shown with arrows. The area corresponding to the MMNm response is shaded.

spectively. In addition, the sustained potential/field (SP/SF) lasts throughout the duration of the stimulus.

Event-related responses can be used to study noninvasively information processing in the brain [54, 56, 80]. With different experimental setups, cognitive neuroscientists try to localize their generator mechanisms in the brain and to reveal the relation of these deflections to different stages of information processing.

3.1 The P50(m) response

The generators of the P50(m) (sometimes termed P1) have been found by intracranial [49] and MEG [32, 50, 100] recordings to be in the supratemporal cortex. Patients with extensive bilateral lesions of the superior temporal cortices, however, have been shown to have intact P50 responses [103], suggesting subcortical subgenerators of P50(m).

3.2 The auditory N1(m) and P2(m) responses

The N1(m) reflects activity of several cerebral sources [56]. Auditory-cortex generators were first suggested on the basis of EEG [94] and confirmed by MEG recordings [28]. Further, with long inter-stimulus intervals, a sensory-modality non-specific component may contribute to the N1(m) response [30, 56]. Finally, evidence of a frontal N1(m) component has been presented [21].

It has been found that in cases when the N1(m) response has been elicited, the stimulus has typically also been consciously detected by the subject, i.e., the elicitation of the N1(m) has been linked to a sensory event, detection [73].

The P2(m) seems to have a non-specific source [95] and an auditory-cortex component [32]. The cognitive functions it reflects are not yet understood.

3.3 The mismatch response

After an occasional deviant tone is presented among a series of identical auditory stimuli, the mismatch response, MMN(m), can be observed [53]. An example of this response is presented in Fig. 3, shaded area. This response begins during the N1(m) but peaks later, typically 100–200 ms after stimulus onset. MMN(m) is most easily seen by subtracting the response to the standards from that to the deviants. The use of the subtraction method is based on the assumption that the basic responses to the standards and the deviants are otherwise the same in this condition. When this assumption is not fullfilled, other techniques can be used [81, 82]. MMN(m) can be recorded even in the absence of attention [55], although strongly focused attention may affect the size of the response [55, 92, 101, 102].

Several locations of origin have been suggested for the MMN(m) [4]. The most prominent component of MMN(m) is located in or near the auditory cortex [5, 26, 29], and it has been suggested to reflect attention-independent change-detection [60]. The frontal MMN(m) component [7, 22, 89] might reflect the brain mechanisms aiming at an involuntary attention switch to sound change [59].

According to a view first presented by Näätänen [57], the neural mechanisms reflected by MMN(m) might be those underlying the human auditory sensory memory. According to this view, the features of the repetitive stimulus are stored in an auditory memory trace and the features of the new sensory input are automatically compared with the trace. When the features of the deviant do not match with the memory trace of the standard, the MMN(m) is elicited. The temporal characteristics of the trace are similar to those reported for the auditory sensory memory, termed *echoic memory* [64].

Since MMN(m) is observed even in the absence of attention or any task to the subject, it is possible to measure this response also in patients who are unable to respond in a typical memory test, and thus several clinical applications of general evaluation of cortical function are being investigated.

With the MMN(m), one can objectively measure the representation accuracy of the sensory memory. For example, in the evaluation of cochlear implants, MMN(m) makes it

possible to study not only whether a sound is perceived but also whether it is discriminable from another sound [45, 82]. Central hearing disorders of newborns have also been explored using MMN(m) [6, 13]. As an index of central deficit in auditory memory, MMN(m) has been used in studies of Alzheimer's disease patients [75, 76]. The use of the MMN in the prognosis of the state of comatose patients has shown promising results [42].

3.4 Responses reflecting active stimulus discrimination

When the subject is paying attention to the stimuli (e.g. giving a response to each deviant or counting the number of deviants), a complex of multiple responses is elicited as a response to the target stimuli. The most prominent peaks in this complex are the N2 and P3 responses. The N2b [58, 60, 86], which forms the N2 together with MMN(m), is apparently related to active stimulus monitoring and reflects discrimination and/or decision-making processes.

The P3 deflection [90] has been proposed to reflect various processes related to decision-making, memory, and/or orienting [18, 83]. The P3 deflection does probably not reflect the activity of a single localized cerebral event since multiple generators have been observed at the P3 latency [9, 26]. Deep or radial sources seem to contribute to the P3 deflection since no reports of a magnetic P3m have been published.

4 Methods for analysing electromagnetic brain responses

The MEG measurements for this thesis were performed using the 24-channel magnetometer of the Low Temperature Laboratory, Helsinki University of Technology and the 122-channel Neuromag magnetometers of the Low Temperature Laboratory and the BioMag Laboratory, Helsinki University Central Hospital. The measurements were performed in magnetically shielded rooms [44, 70].

The Neuromag-122 magnetometer covers the whole scalp, thus allowing one to measure brain activity from both hemispheres and all lobes simultaneously. This is an essential improvement in MEG technology – in previous instruments, a set of 24–37 channels had to be placed successively on different areas of the head surface in order to cover a larger area for more accurate source localization.

Superconducting quantum interference devices (SQUIDs) are used to detect small changes in the magnetic field. The external flux is applied to the SQUID via the input coil attached to a flux transformer placed

as near to the brain as possible. The pickup coils in the Neuromag magnetometer are first-order planar gradiometers [61], which are sensitive to tangential derivatives of the magnetic field.

4.1 Interpreting electric potentials and magnetic fields

The current density $\mathbf{J}(\mathbf{r})$ can be thought of consisting of the volume current $\mathbf{J}^v(\mathbf{r})$, which is passive current as the result of electric field in the tissue, and of the primary current $\mathbf{J}^p(\mathbf{r})$. To determine the primary current $\mathbf{J}^p(\mathbf{r})$ in the brain on the basis of the electric potential and the magnetic field measured outside the brain is called the *bioelectromagnetic inverse problem*. In order to obtain a unique solution to the inverse problem, a model of the conductive volume and the source are needed.

It can be safely assumed that primary currents arise only in brain tissue. The brain can be modelled with a sphere whose surface fits as closely as possible to the local interior skull surface [37]. In all studies included in this thesis, a spherical volume-conductor model was used. For more accurate results, three-dimensional mesh reconstructions of the brain and head surfaces are increasingly being applied [16, 105].

Anatomical data from computerized tomography, CT, or magnetic resonance imaging, MRI [69], are important in functional imaging; when the functional information is superimposed on the anatomical image, the location of the source can be compared to the structural details of the brain [33]. Anatomical images are also needed in accurate EEG and MEG source modeling: the sphere best fitting the local interior skull surface or 3-dimensional mesh rendering of the surfaces for modeling the conductive materials [38] can be constructed on the basis of the anatomical images.

In selecting a source model, however, several things should be considered. All possible a priori information on the characteristics of the source should be taken into account in the choice of the model. If small source areas are expected, as in the case of the earliest somatosensory responses [69], non-linear dipolar models can be applied. If the sources are more wide-spread, as in Publication III, linear methods like minimum-norm estimates or lattices of dipoles are more appropriate to depict the spatio-temporal behaviour of the currents. When only the temporal behaviour of sources characterized by known field patterns are needed, linear projection methods can be used without modeling the current distribution or the volume conductor.

In addition to the MEG data analysis methods developed in this thesis, several modifications of old techniques and a few novel methods have been developed. PET and fMRI data are increasingly used

as constraints to the electromagnetic source models. Low resolution brain electromagnetic tomography, LORETA [74], is a new, still controversial technique for solving the inverse problem without assuming restricted sources. Spatiotemporal MNLS inverse [97] and FOCUSS [24] are other new methods to estimate a continuous current distribution. Brain electromagnetic source analysis, BESA [88], and current reconstruction and imaging framework CURRY [1] offer, in addition to minimizing variance, also other criteria for restricted source (dipole) fitting and a multitude of linear data visualization and analysis techniques.

4.2 Minimum-norm estimate

The minimum-norm estimate (MNE) [34, 35, 36, 41, 87] is a continuous estimate of the primary current $\mathbf{J}^p(\mathbf{r})$ in the brain confined to a specified volume.

A vector field $\mathbf{L}_i(\mathbf{r})$ describing the spatial sensitivity of a detector to primary currents can be defined as

$$B_i = \int \mathbf{L}_i(\mathbf{r}) \cdot \mathbf{J}^p(\mathbf{r}) dv, \qquad (1)$$

where B_i is the output of the ith detector. The MNE, an estimate $\mathbf{J}^*$ of the primary current $\mathbf{J}^p$, is a linear combination of the lead fields of the detectors,

$$\mathbf{J}^* = \sum_{i=1}^{n} \omega_i \mathbf{L}_i, \qquad (2)$$

where ω_i are scalars determined by the signals of the detectors in each measurement.

We assume that the estimate $\mathbf{J}^*$ reproduces the measured field values

$$b_i = \int_G \mathbf{L}_i(\mathbf{r}) \cdot \mathbf{J}^*(\mathbf{r}) dG, \qquad (3)$$

where G is the volume into which the estimate is confined to. Combining (3) and (4) we get a set of linear equations

$$\mathbf{b} = \mathbf{\Pi}\mathbf{w}, \qquad (4)$$

where $\mathbf{b} = (b_1, ..., b_n)^{\mathrm{T}}$, $\mathbf{w} = (w_1, ..., w_n)^{\mathrm{T}}$, and $\mathbf{\Pi}$ is a matrix containing the inner products of the lead fields.

The use of the MNE requires only the assumption of a current region G. It is the current distribution with the smallest norm

$$||\mathbf{J}^p||^2 = \int_G |\mathbf{J}^p(\mathbf{r})|^2 dG \qquad (5)$$

that is capable of explaining the measured signals.

The MNE is the best estimate of the primary current in cases when the a priori information of the distribution of the primary current is limited to knowledge about the source volume. In a simple case, the surface of a sphere is used, but in more sophisticated examples one can use a reconstruction of the cortical foldings of the brain or areas found to be

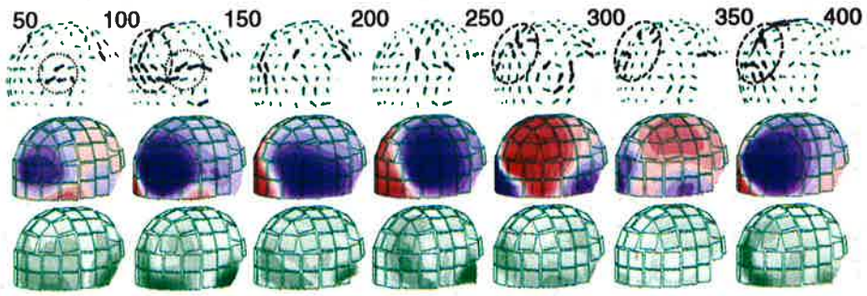

Figure 4: **Right-hemisphere responses of SK, a blind subject from Publication III, to deviant tones in an active discrimination condition are shown in 50-ms steps, with frontal areas to the right. Upper row: The MNE is depicted with arrows. Notice the strong temporal and occipital activity circled with dotted and dashed lines, respectively. Middle row: Magnetic field isocontour maps showing the magnetic field entering (blue) and coming out of the head (red). Lower row: Magnetic field gradient isocontour maps showing the strongest gradient above the source with dark green.**

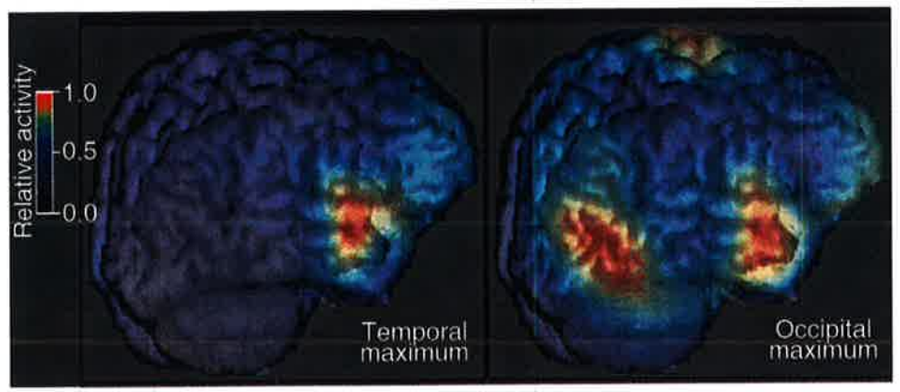

Figure 5: **Temporal (left) and occipital (right) maxima were chosen for the MNE of the primary current distribution. The values of the primary current are presented with colour scaling projected onto a three-dimensional triangular mesh of the subject's brain surface on top of a rendering of the cortical surface. Figure from Publication III.**

active with methods measuring brain metabolism.

Examples of the MNEs calculated on the surface of a sphere are presented in Fig. 4 (upper row). Samples of the continuous MNE are presented with arrows, whose direction and size correspond to the direction and strength of the estimated primary current.

The MNE is an unstable estimate without regularization [87] which is a technique suppressing those components of the estimate that are not detected strongly by the sensors. This can be done by ignoring the noise-dominated components of the estimate or, more optimally, by weighting the components for example according to their signal-to-noise ratios [65].

Minimum-norm estimation was related to brain anatomy in Publication III in a new way; the MNE was computed on a spherical surface and projected onto a three-dimensional mesh of the cortical surface. For visualization, the continuous MNE is typically sampled and the current direction and strength of each sample is presented with an arrow, see Fig. 4. We chose to present the results in the form of a color-coded map, see Fig. 5, thus presenting only the strength information without the direction information. Calculating the MNE on the mesh reconstruction would increase accuracy of the result, since the choice of the volume G affects the results.

Prior to dipole fitting in Publications I, II, IV, VI, and VII, the MNE was used for visual inspection of the data. The MNE was computed on a spherical surface fitting closely to the local cortical curvature. The MNE was used to confirm that the number of dipoles corresponded to the number of current maxima in the estimate.

4.3 Single- and multiple-dipole models

In order to justify the use of a current dipole as a source model one must assume that the activity is generated by a current in a small source area containing a dipolar term so that its magnetic field can be closely approximated by that of a point-like current dipole. Radial sources do not generate a magnetic field outside a spherically symmetric conductor, and thus only tangential dipoles are used with the spherical model for MEG data interpretation. A tangential dipole has five parameters: three for the location, one for the direction, and one for the strength of the current flow. These parameters can be determined numerically by a least-squares fit.

The parameters for a small number of dipoles can be fitted by selecting, separately for each source, first, the temporal range where it is most active compared with other sources, and second, the channel combination which shows the double-lobed dipolar field pattern elicited by this source simultaneously

trying to avoid contamination from other sources. Using these as initial values, an iterative fit of the locations, orientations, and/or strengths can be performed taking into account data from all channels and all time points during the active periods of the sources.

If the activity of several sources overlaps in time, the accuracy to locate sources increases with increasing spatial separation. If many sources are active close to each other and also in temporal synchrony, dipole modelling is not sufficient for separating or even locating the sources. Also, if the number of data-explaining dipoles differs from the number of actual sources, the dipole locations may be incorrect.

The goodness-of-fit value, g, is a measure of how similar the field pattern caused by the equivalent current dipole and the measured field pattern are [43]. This is given by

$$g = 1 - \left(\sum_{i=1}^{n} b_i^2 \right)^{-1} \sum_{i=1}^{n} (b_i - \hat{b}_i)^2, \quad (6)$$

where b_i are the experimental data, n is the number of channels, and $\hat{b}_i$ are the field values calculated using the equivalent current dipole.

In practice, more than 20 channels are needed for a non-biased dipole location estimation, and the fit can be considered to justify the use of a dipole when the goodness-of-fit is over 70%. Increasing the number of channels reduces the goodness-of-fit value since more data will simultaneously introduce more noise.

In Publications I, II, IV, VI, and VII, the dipole model was used as a source model. In Publication I, the dipole model explained 69–99% of the field variance at 24 channels. The source strengths varied from 8 to 23 nAm (average of 9 subjects). With only 24 channels, one-dipole fitting was in practice the only possibility for point-like source localization.

In Publication II, the magnetic field was measured with the 24-channel magnetometer from two overlapping locations. This increased the accuracy to locate sources by revealing the field distribution from a wider area, and revealed the subtle tonotopical changes in the current direction.

In Publication IV, the magnetic field was measured with 122 channels over the head; dipole modelling was used to locate the sources. More than 200 epochs of MEG were averaged for all stimulus classes and the dipole model explained more than 85% of the field variance at 44 channels centered around the auditory cortex. Since the head position in the two conditions or the estimated source locations for the responses to the frequency change did not differ significantly, the measured field gradient values from the channel showing the largest response were used as estimates of the source strengths in addition to the dipole moments. In this case, these two analysis methods produced relatively similar results; 33 and 49% reduction in source strength.

In Publication VI, as in Public-

ation II, the source current direction was a more robust indicator of tonotopy than the source location estimated with a current dipole. In Publication VII, a systematic ampliotopic change was observed in source locations when estimated with current dipoles. The stimulus presentation rate was high in order to maximize the interaction between different stimulus intensities. This, however, yielded small responses, low signal-to-noise ratios, and low goodness-of-fit values. For this reason, a model of cortical refractoriness was formulated and the ampliotopy was successfully confirmed with both magnetic field gradient values and dipole moments.

4.4 The signal-space projection method

In studies of the temporal behavior of neuronal sources, the signal-space projection method, SSP [91, 93], is applicable in the analysis of both spontaneous and evoked MEG and EEG data elicited by both spatially distributed and well-localized neuronal sources.

The measured signals can be represented as a time-dependent vector $\mathbf{M}(t)$ in an n-dimensional signal space, where n is the number of channels of the measurement device; each component of $\mathbf{M}(t)$ correspond to one channel in the measurement. Each EEG and MEG channel measures a weighted sum of activity of the sources in the brain. Thus, vectors in the n-dimensional signal space correspond to source configurations, i.e., to the time-independent location and direction information of the sources in the brain.

The SSP method can be used for identifying N sub-populations of sources with time-independent spatial distributions, which are determined as vectors in the signal space. When the strengths of these sources vary in time, the amplitudes of the signal vectors vary proportionately.

The signal vector $\mathbf{M}(t)$ can be expressed as

$$\mathbf{M}(t) = \sum_{i=1}^{N} a_i(t)\mathbf{s}_i + \mathbf{n}(t), \qquad (7)$$

where vectors $\mathbf{s}_i$ are unit vectors characterizing the sources and can be referred to as components of the signal in the signal space. The coefficients $a_i(t)$ describe the temporal behavior of the sources; $\mathbf{n}(t)$ is noise from other, simultaneous brain activity and from extracerebral sources. For each source i, the corresponding source vector $\mathbf{s}_i$ defines the shape of the field pattern produced by this source; each component of $\mathbf{s}_i$ indicating the signal values measured by the different sensor channels.

If the temporal behavior of the sources contributing to the measured data is to be studied, the vectors $\mathbf{s}_i$ can be determined as field patterns of interest e.g. at peak latencies of evoked responses, assuming that the field pattern remains the same over time. On the other hand, if activity in given brain areas is of interest, vectors $\mathbf{s}_i$ can be obtained by calculating the field pattern generated by sources in the regions of interest. In practice, when determining the vectors $\mathbf{s}_i$ from the measured data, it is useful to restrict the set of channels to those in which the signal exceeds the noise level [91].

After determining the vectors $\mathbf{s}_i$, the N-dimensional vector $\mathbf{a}(t) = [a_1(t), a_2(t), ..., a_N(t)]^{\mathrm{T}}$ describing the temporal behavior of the sources is to be determined. Equation (7) can be written as follows:

$$\mathbf{M}(t) = \mathbf{S}\mathbf{a}(t) + \mathbf{n}(t), \qquad (8)$$

where the source matrix $\mathbf{S} = (\mathbf{s}_1, \mathbf{s}_2, ..., \mathbf{s}_N)$ is independent of time. If the expectation value $E\{\mathbf{n}(t)\} = 0$, an unbiased estimate for $\mathbf{a}(t)$ is

$$\mathbf{a}(t) = \mathbf{S}^{+}\mathbf{M}(t), \qquad (9)$$

where $\mathbf{S}^{+} = [\mathbf{S}^{\mathrm{T}}\mathbf{S}]^{-1}\mathbf{S}^{\mathrm{T}}$ is the pseudoinverse of $\mathbf{S}$. For each source vector corresponding to the sources selected, this estimate describes the source waveforms as a function of time (for an example, see Fig. 7). In contrast to dipole modeling, the signal-space projection method gives an estimate of the source strength also when the source is weak. With weak sources, the dipole model typically fails to explain the measured data successfully giving no useful estimate of the source strength.

A component of the signal space can be projected out of the data in order to reveal other sources. The projected-out signal space is orthogonal to the source or set of sources. This allows investigation of data without the contribution of the projected-out source, and thus may make dipole modelling or other source estimation possible in some cases. Evidently, the projection operation must be taken into account in modelling calculations when source modelling is performed on data left after the projection. Unfortunately, data misinterpretation is evident if the projected-out source is picked with distortion or is not stable over time.

In Publication V, SSP was used to reject epochs containing eye-blink artefacts. The magnetic field pattern at the peak of the average of a few eye blinks was selected as a representative of an eye-blink source vector. When during an epoch the angle between the measured signal vector and the eye-blink vector was below a rejection criterion, the epoch was rejected from the ERF average. The rejection according to SSP was in good agreement with rejection according to traditional methods using EOG rejection.

The use of SSP in correcting data containing eye-blink artefacts was also demonstrated in Publication V. The auditory ERF was revealed after eye-blink suppression with SSP. This method saves even more time than eye-blink rejection with SSP, because almost all epochs can be used in the average. After the suppression, however, sources with similar field distributions to an eye-blink artefact can not be studied.

5 Comparative source analysis

In this Section, examples of the use of the MNE, multidipole models, and the SSP in analyzing brain activation data are presented and these analysis methods are compared with each other. The data used are from Subject SK in Publication III.

5.1 Minimum-norm estimation

In Publication III, auditory event-related MEG data from blind and sighted subjects were presented. Plasticity of the human brain, i.e., the ability of the brain to reorganize and adapt to changing conditions, was studied by presenting standard and deviant tones in the *passive* (subjects were reading) and *active* (subjects were counting the deviant stimuli) conditions. In the active condition, in the blind subjects, prominent activity was observed in the parieto-occipital areas of the brain. The responses were analyzed using unweighted MNEs calculated on the surface of a sphere which was fitted as closely as possible to the subject's brain in temporal, parietal, and occipital areas. The result was then projected onto a triangular mesh reconstruction of the brain surface, see Fig. 5.

The MNE was derived from the deviant response at the latencies of the maximum activity in the temporal and occipital sensors, 140 and 330 ms, respectively, for this subject. Because of limited space in the journal, the relation of these data to the known peaks of the auditory evoked response, the P50m, the N1m, the MMNm, the N2b, and the P3, was not discussed in Publication III. These peaks can be recognized by studying their temporal behavior and location of origin.

In the passive condition, the P50m, the N1m, the P2m, and the MMNm evoked responses are expected during the time period 30–200 ms (see Fig. 3). In the active condition, the P50m, N1m, and MMNm responses were also present as in the reading condition. Systematic attentional modulation [27, 53] was not observed in this subject. Additional deflections, however, were observed over the parieto-occipital areas.

By calculating the MNE in steps of 10 ms and inspecting the estimated current distribution in the occipital areas, it was possible to study the strength, direction, and temporal behavior of the additional sources. The MNEs of the response to the deviants in the active condition are presented in steps of 50 ms in Fig. 4, showing parieto-occipital activity starting already at 150 ms after the stimulus onset. In this early phase, the direction of the current was from right occipital areas towards left parietal areas. The strength of the activity was approximately the same as in the auditory cortex provided that the depths of the two sources were the same.

There is a reduction of amplitude in the MNE at the parieto-occipital area at about 200 ms. After this, a strong signal from a parieto-occipital location appears, lasting from 250 to 450 ms. The direction of this current is from the occipital areas towards the parietal regions, also mainly from right to left.

To conclude, according to MNE, parieto-occipital areas were activated in this blind subject, when a deviant (target) stimulus was presented in the active condition. There seem to be two sources of attention-related activity in the parieto-occipital areas. The sources are separated by their time behaviors and by their slightly different orientations. There seems to be a minor difference also in the location of the source; the later component seems to be located closer to the parietal areas.

5.2 Dipole modelling

The magnetic field and gradient maps of the deviant response of Subject SK in the active condition are displayed in Fig. 4 in steps of 50 ms for demonstration purposes. The gradient maps show some contribution from the parieto-occipital cortex as early as 100 and 150 ms after stimulus onset. At latencies from 200 to 400 ms, a strong, clearly nondipolar field distribution can be observed in the occipital areas.

In the auditory areas, a dipolar (double-lobed) field distribution can be observed at the latencies of the P50m and the N1m in the responses to the standard tone and at the latency of the MMNm in the subtraction curve (the mapping was done in 10 ms steps). To model the sources of these responses, a current dipole was fitted by selecting 44 channels centered around the auditory cortex. This number of channels is large enough to get an unbiased estimate of the source location, while containing no contribution from the other source area in the opposite hemisphere.

A sphere, fitting as close as possible to the temporal, parietal, and occipital cortical surfaces of this subject, was used as the volume model. The dipoles in the auditory cortices were able to explain 82–95% of the variance of the measured data above the auditory cortex (see Table) in the passive condition and 79–95% in the active condition (Fig. 6). During the MMNm, a contribution from the parieto-occipital sources presumably reduced the goodness-of-fit value. The occipital and parietal activity in the active condition was left unexplained by the auditory-cortex dipoles.

An attempt was made to explain the parieto-occipital activity with a single current dipole. Since the source does not seem to be localized,

Results of dipole modelling					
Source name		Passive condition		Active condition	
and location		peak [ms]	g [%]	peak [ms]	g [%]
P50m	right temporal	47	89	46	89
P50m	left temporal	49	89	47	89
N1m	right temporal	109	94	98	94
N1m	left temporal	98	95	102	95
P2m	right temporal	212	84	216	84
P2m	left temporal	208	87	212	87
MMNm	right temporal	142	85	132	79
MMNm	left temporal	149	82	139	83
N2b	parieto-occipital			180	47
P3	parieto-occipital			300	38

Table 1: Results of dipole modelling show that sources in the right and left temporal cortices explain 79–95% of the measured data over the temporal cortices. The sources in the occipital cortex, however, explain less than 50% of the data, which can be considered as an indicator of a more widespread source area.

it is not surprising that the model failed to explain the measured data seen in the parieto-occipital channels (Fig. 6). This attempt resulted in a very deep source location and unsatisfactorily large variance.

To conclude, with dipole modelling it was possible to estimate the location and orientation of the sources in the auditory cortices during the peaks of the responses. The location, strength, and temporal behavior of the occipital and parietal sources, however, could not be estimated using dipole modelling.

5.3 Signal-space projection

In the responses to the deviants, the strength of the right and left temporal-cortex sources peaked at 129 and 120 ms, respectively, after the stimulus onset. The field patterns at these latencies were picked as source vectors $\mathbf{s}_r$ and $\mathbf{s}_l$ to characterize temporal-cortex activity. The field pattern for the signal vectors was chosen at 64 channels over the right and left hemispheres. The contribution of these sources was projected out of the data measured in the active condition.

The parieto-occipital sensor showed a strong response peaking as early as 180 ms after stimulus onset, suggesting a possible contribu-

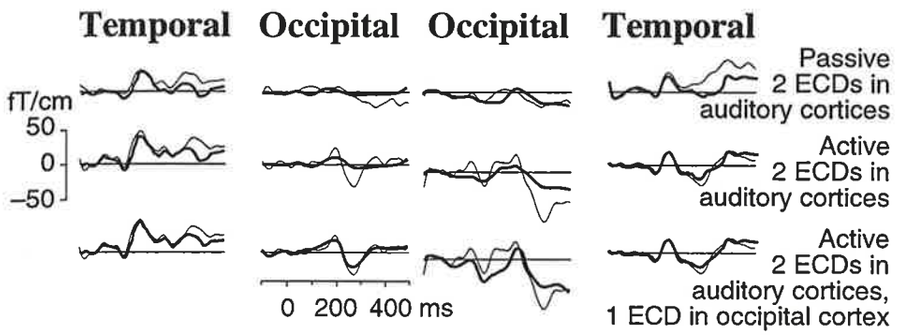

Figure 6: Original measured responses to deviant tones (thin line) and dipole explanation (thick line) for one dipole in each auditory cortex in the passive (upper) and active (middle row) condition. The last row shows the case for a three-dipole fit including an additional occipital dipole in the active condition.

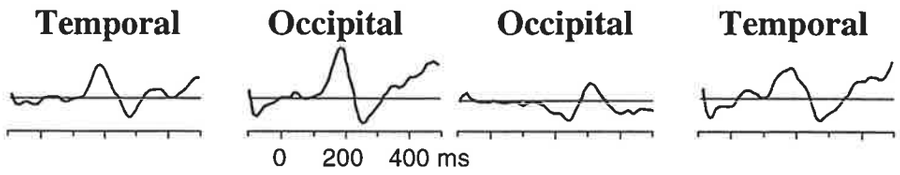

Figure 7: Temporal behavior of the temporal (left and right) and occipital sources (middle columns) in the active condition was found by choosing projection operators from the left and right temporal cortex and the two occipital cortex maxima.

tion from the N2b component. This hypothesis is also supported by previous EEG findings of evoked responses from blind subjects in active discrimination conditions [47]. The field pattern at 180 ms was picked as source vector $\mathbf{s}_{o1}$ using 56 parieto-occipital channels and projected out of the data.

After the projection, another parieto-occipital response remained in the data peaking at about 260 ms after stimulus onset. The field pattern was picked as source vector $\mathbf{s}_{o2}$ using 56 parieto-occipital channels.

After projecting out the activity characterized by these four source vectors, only noise was left in the remaining data. To conclude, according to SSP, the parieto-occipital responses, although widespread, are characterized by two stable field distributions over time, peaking at 180 and 260 ms after stimulus onset.

5.4 Comparison of source-analysis methods

The stepwise MNE (Fig. 5) presents the whole temporal pattern of the primary current. This is the most straightforward way of examining the data because no assumptions are made about the number or location of sources. Accuracy is increased if the MNE is calculated on a three-dimensional mesh rendering of the cortical surface. Even when calculated on a spherical surface, the MNE used in conjunction with a three-dimensional reconstruction of the brain surface can provide information on the approximate location and temporal behavior of sources. This method can also be used as a starting point of data analysis — the number and type of sources can be estimated before moving into more localized source models.

Dipole modelling gives a highly accurate source location when point-like sources are far away from each other or the sources have a separate temporal behavior. For widespread sources, arrangements of dipoles in layers could be used, but the use of a single dipole results in an unsatisfactorily large variance and thus the parameters of such a dipole may be misleading.

The projection method allows data analysis without assumptions about the source distribution. Thus all stable field configurations can be used to characterize neuronal sources. The stability of the field distribution can be verified by projecting its contribution out of the data and studying the complement. If the sources are moving or changing their orientation over time, SSP distorts the data and does not provide reasonable results. Also, if the field pattern selected to characterize a source contains contribution from several sources with different time behaviours, the result of SSP is meaningless.

From the set of data analyzed above, the MNE and the SSP were able to determine the existence and time behavior of the two distinct parieto-occipital sources, while dipole modelling was unsuccesful. The approximate location of these sources was revealed with the MNE only; dipole modelling failed because of distributed sources and SSP does not give estimates source locations. The location of the point-like auditory-cortex sources was given accurately by dipole modelling and approximately by MNE. The temporal behavior of the auditory-cortex sources was revealed with all three methods.

6 Conclusions

A comparison of three data analysis methods was presented in Section 5. All these analysis methods, the MNE, dipole model, and SSP, were able to bring valuable information on the sources eliciting the data. The MNE revealed the temporal and approximate spatial characteristics of the neuronal currents. The dipole model was able to reveal the location of the temporal sources. SSP showed that the occipital activity can be characterized by two signal vectors. Thus all of these methods are important in studying complex field patterns produced by multiple neuronal sources.

By studying auditory event-related magnetic fields, it is possible, after revealing the basic steps of auditory information processing, to explore higher cognitive functions. By using the mismatch response, we can study perception accuracy and sensory memory without any task for the subject. Voluntary actions and language functions can be studied with attention paradigms.

Cognitive studies are clearly more demanding than those related to basic information processing. First, multiple and possibly widespread source areas are active simultaneously. This requires the use of more sophisticated source models than a single dipole. More importantly, the design of experimental paradigms becomes even more essential. The cognitive brain activity must be separated from basic processing already at the level of experimental design.

List of Publications

I Kimmo Alho, Minna Huotilainen, Hannu Tiitinen, Risto J. Ilmoniemi, Jukka Knuutila, and Risto Näätänen: Memory-related processing of complex sound patterns in human auditory cortex: a MEG study. *NeuroReport* **4** (1993) 391-394.

II Hannu Tiitinen, Kimmo Alho, Minna Huotilainen, Risto J. Ilmoniemi, Juha Simola, and Risto Näätänen: Tonotopic auditory cortex and the MEG equivalent of the mismatch negativity. *Psychophysiology* **30** (1993) 537–540.

III Teija Kujala, Minna Huotilainen, Janne Sinkkonen, Antti Ahonen, Kimmo Alho, Matti S. Hämäläinen, Risto J. Ilmoniemi, Matti Kajola, Jukka E. T. Knuutila, Juha Lavikainen, Oili Salonen, Juha Simola, Carl-Gustav Standertskjöld-Nordenstam, Hannu Tiitinen, Satu O. Tissari, and Risto Näätänen: The visual cortex of blind humans participates in auditory discrimination. *Neuroscience Letters* **183** (1995) 143–146.

IV Minna Huotilainen, Risto J. Ilmoniemi, Juha Lavikainen, Hannu Tiitinen, Kimmo Alho, Janne Sinkkonen, Jukka Knuutila, and Risto Näätänen: Interaction between representations of different features of auditory sensory memory. *NeuroReport* **4** (1993) 1279–1281.

V Minna Huotilainen, Risto J. Ilmoniemi, Hannu Tiitinen, Juha Lavikainen, Kimmo Alho, Matti Kajola, Juha Simola, and Risto Näätänen: The projection method in rejecting eye-blink artefacts from multichannel MEG measurements. In: *Biomagnetism: Fundamental research and clinical applications* Editors: C. Baumgartner, L. Deecke, G. Stroink, and S. J. Williamson (1994) 363–367.

VI Minna Huotilainen, Hannu Tiitinen, Juha Lavikainen, Risto J. Ilmoniemi, Eero Pekkonen, Janne Sinkkonen, Petteri Laine, and Risto Näätänen: Sustained fields of tones and glides reflect tonotopy of the auditory cortex. *NeuroReport* **6** (1995) 841–844.

VII Minna Huotilainen, Janne Sinkkonen, Hannu Tiitinen, Risto J. Ilmoniemi, Eero Pekkonen, Lauri Parkkonen, and Risto Näätänen: Intensity representation in the human auditory cortex. *TKK Report series of the Laboratory of Acoustics and Audio Signal Processing* **42** (1997) 1–4.

7 Summary of Publications

In all of these publications, the first author was responsible for the experimental setup and writing of the manuscript. I have participated in the development of the stimulation systems, planning of the measurement setups, collection of data, analysis and modelling of data, and editing of the manuscripts of all of these seven publications. I was responsible, together with Janne Sinkkonen, for the data analysis and display methods in Publications III and VII. In Publications IV–VII, my coauthors collaborated mostly in the form of comments on the manuscript.

I Memory-related processing of complex sound patterns in human auditory cortex: a MEG study

Responses to complex sound patterns consisting of 9 successive 50-ms segments of different frequencies were recorded with a 24-channel magnetometer above the right temporal cortex. The frequency of one of the segments was changed in 20% of the stimuli. This change elicited a mismatch response peaking about 200 ms after the onset of the deviating segment. Current dipoles were used to model the sources of these responses; they were found to be located in the auditory cortex.

II Tonotopic auditory cortex and the magnetoencephalographic (MEG) equivalent of the mismatch negativity

Responses to two tone stimuli, a frequently presented standard stimulus and an infrequent deviant stimulus, were recorded with a 24-channel magnetometer. The recordings were performed in two partially overlapping locations over the anterior and posterior temporal cortex of the right hemisphere. Standard tone frequencies of 250, 1000, and 4000 Hz were used with corresponding deviants of 275, 1100, and 4400 Hz in different blocks. The most prominent responses were the N1m and the MMNm responses. The modeling of the responses with equivalent current dipoles showed that the MMNm source is anterior to that of N1m. The dipole orientations of both N1m and MMNm sources depended on stimulus frequency, suggesting that both responses are generated in a tonotopically organized areas.

III The visual cortex of blind humans participates in auditory discrimination

MEG measurements of blind subjects in an auditory active discrimination condition revealed that in addition to temporal areas, parieto-occipital areas of the blind contribute to the discrimination of auditory stimuli. The activity seen in the occipital and parietal areas of these blind subjects demonstrates the plasticity of the human brain. The MNE was used to display an estimate of the primary current on a three-dimensional surface of the brain. The MNE was computed on a spherical surface fitted closely to each subjects' brain surface in temporal, parietal, and occipital lobes, and projected onto a three-dimensional mesh of the surface of the brain. The result was displayed as a colour-coded map on top of the renderings of the subjects MR images.

IV Interaction between representations of different features of auditory sensory memory

In this study, the organization of the auditory sensory memory related with the mismatch response was studied by developing an experimental condition in which only one feature was common to the otherwise varying, multiple standard stimuli. The sources were modelled with equivalent current dipoles and the source strength estimation was done using the dipole strengths. The importance of this feature (frequency) was demonstrated by the fact that varying the other features did not prevent the frequency change detection system, that is, the mismatch response was generated also in this condition. The varying features, however, affected the response in a significantly attenuating manner, suggesting either that the frequency-change detection system can be affected by the other, constantly active change-detection systems, or overlapping of features in the memory trace.

V The projection method in rejecting eye-blink artefacts from multichannel MEG measurements

The ability of the spatial filter used in the projection method to eliminate the eye-blink artefact from auditory-response data was presented. By using the signal-space projection method (SSP), epochs contaminated with eye blinks can be either searched for and removed from the average, or the contamination of the eye blinks can successfully be projected out of the average in order to reveal the auditory response.

A spatial filter from a characteristic pattern present in the blink was capable of characterizing the source with a chosen spatial distribution as a function of time. This filtering method discriminated against all other possible sources without the specification of the distribution of the selected source, and thus the method can be used for both distributed and localized sources.

VI Sustained fields of tones and glides reflect tonotopy of the auditory cortex

In this study, auditory stimuli lasting 700 ms were used to evoke the sustained-field activity in addition to the N1m response for examining the tonotopy of the two responses. Both constant- and varying-frequency stimulation was used in order to differentiate between the sustained field and the N1m activity. Both responses showed tonotopy, and, in the case of the sustained field, the frequency pattern of the stimulus was reflected in the relative angle of the sustained field. The sources were modelled with current dipoles, and the tonotopy was revealed both in the location and the direction information of the sources.

VII Evidence for intensity-specific neurons in the human auditory cortex

Tones with varying intensity were presented in rapid succession. The N1m response was modelled with a current dipole whose amplitude was found to vary nonmonotonically as a function of intensity. This finding can be explained by an ordered representation of intensity on the cortex. This explanation was also supported by the systematic location change found in the sources. A model was proposed for estimating the size of the cortical area affected by a single stimulus. This model is applicable for investigating other feature-specific cortical neuronal populations.

References

[1] *User Guide CURRY Version 2.1.* Philips Electronics N.V., Eindhoven, Netherlands, 1996.

[2] JC Adams. Neuronal morphology in the human cochlear nucleus. *Arch Otolaryngol*, 112:1253–1261, 1986.

[3] AI Ahonen, MS Hämäläinen, MJ Kajola, JET Knuutila, P Laine, OV Lounasmaa, JTA Simola, and CD Tesche. A 122-channel SQUID instrument for investigating the magnetic signals from the human brain. *Phys Scripta*, T49:198–205, 1993.

[4] K Alho. Cerebral generators of mismatch negativity (MMN) and its magnetic counterpart (MMNm) elicited by sound changes. *Ear Hear*, 16:38–51, 1995.

[5] K Alho, P Paavilainen, K Reinikainen, M Sams, and R Näätänen. Separability of different negative components associated with auditory stimulus processing. *Psychophys*, 23:613–624, 1986.

[6] K Alho, K Sainio, N Sajaniemi, K Reinikainen, and R Näätänen. Event-related brain potential of human newborns to pitch change of an acoustic stimulus. *Electroenceph clin Neurophys*, 77:151–155, 1990.

[7] K Alho, DL Woods, A Algazi, RT Knight, and R Näätänen. Lesions of frontal cortex diminish the auditory mismatch negativity. *Electroenceph clin Neurophys*, 91:353–362, 1994.

[8] JA Assad, GMG Shepherd, and DP Corey. Tip-link integrity and mechanical transduction in vertebrate hair cells. *Neuron*, 7:985–994, 1991.

[9] P Baudena, E Halgren, G Heit, and J Clarke. Intracerebral potentials to rare target and distractor stimuli. III. Frontal cortex. *Electroenceph clin Neurophys*, 94:251–264, 1995.

[10] O Bertrand, F Perrin, and J Pernier. Evidence for a tonotopic organization of the auditory cortex observed with auditory evoked potentials. *Acta Oto-Laryngol*, 491:116–122, 1991.

[11] JF Brugge and MM Merzenich. Patterns of activity of single neurons of the auditory cortex in monkey. In A Möller, editor, *Basic mechanisms of hearing*, pages 745–767. Academic Press, New York, 1973.

[12] GG Celesia and F Puletti. Auditory cortical areas of man. *Neurol*, 19:211–220, 1969.

[13] M Cheour-Luhtanen, K Alho, T Kujala, K Sainio, K Reinikainen, M Renlund, O Aaltonen, O Eerola, and R Näätänen. Mismatch negativity indicates vowel discrimination in newborns. *Hear Res*, in press:–, 1996.

[14] DP Corey and AJ Hudspeth. Ionic basis of the receptor potential in a vertebrate hair cell. *Nature*, 281:675–677, 1979.

[15] OD Creuzfeldt, S Watanabe, and HD Lux. Relations between EEG phenomena and potentials on single cortical cells. I. Evoked responses after thalamic and epicortical stimulation. *Electroenceph clin Neurophys*, 20:1–18, 1966.

[16] BN Cuffin. A method for localizing EEG sources in realistic head models. *IEEE Trans Biomed Eng*, 42:68–71, 1995.

[17] P Dallos. Cochlear physiology. *Annu Rev Physiol*, 32:153–190, 1981.

[18] E Donchin and M Coles. Is the P300 component a manifestation of context updating? *Behav Brain Sci*, 11:357–374, 1988.

[19] C Elberling, C Bak, B Kofoed, H Lebech, and K Saermark. Auditory magnetic fields: Source location and tonotopic organization in the right hemisphere of the human brain. *Scand Audiol*, 11:61–65, 1982.

[20] N Geschwind and W Levitsky. Human brain: Left-right asymmetries in temporal speech region. *Science*, 161:186–187, 1968.

[21] MH Giard, F Perrin, and JF Echallier. Dissociation of temporal and frontal activity patterns during the human auditory N1 wave: A scalp current density and dipole model analysis. *Electroenceph clin Neurophys*, 92:238–252, 1994.

[22] MH Giard, F Perrin, J Pernier, and P Bouchet. Brain generators implicated in the processing of auditory stimulus deviance: a topographic event-related potential study. *Psychophys*, 27:627–640, 1990.

[23] JM Goldberg and PB Brown. Functional organization of the dog superior olivary complex: an anatomical and electrophysiological study. *J Neurophysiol*, 31:639–656, 1968.

[24] IF Gorodnitsky, JS George, and BD Rao. Neuromagnetic source imaging wiht FOCUSS: a recursive weighted minimum norm algorithm. *Electroenceph clin Neurophysiol*, 95:231–251, 1995.

[25] A Grinvald, RD Frostig, E Lieke, and R Hildesheim. Optical imaging of neural activity. *Physiol Review*, 68:1285–1366, 1988.

[26] E Halgren, P Baudena, JM Clarke, G Heit, C Liégois, P Chauvel, and A Musolino. Intracerebral potentials to rare target and distractor auditory and visual stimuli. I. Superior temporal plane and parietal lobe. *Electroenceph clin Neurophys*, 94:191–220, 1995.

[27] JC Hansen and SA Hillyard. Endogenous brain potentials associated with selective auditory attention. *Electroenceph clin Neurophys*, 49:277–290, 1980.

[28] R Hari, K Aittoniemi, M-L Järvinen, T Katila, and T Varpula. Auditory evoked transient and sustained magnetic fields of the human brain: Localization of neural generators. *Exp Brain Res*, 40:237–240, 1980.

[29] R Hari, M S Hämäläinen, R J Ilmoniemi, E Kaukoranta, K Reinikainen, J Salminen, K Alho, R Näätänen, and M Sams. Responses of the primary auditory cortex to pitch changes in a sequence of tone pips: neuromagnetic recordings in man. *Neurosci Lett*, 50:127–132, 1984.

[30] R Hari, K Kaila, T Katila, T Tuomisto, and T Varpula. Interstimulus interval dependence of the auditory vertex response and its magnetic counterpart: Implications for their neural generation. *Electroenceph clin Neurophys*, 54:561–569, 1982.

[31] R Hari and OV Lounasmaa. Recording and interpretation of cerebral magnetic fields. *Science*, 244:432–436, 1989.

[32] R Hari, M Pelizzone, JP Mäkelä, J Hällström, L Leinonen, and OV Lounasmaa. Neuromagnetic responses of the human auditory cortex to on- and offsets of noise bursts. *Audiol*, 26:31–43, 1987.

[33] M Hämäläinen. Anatomical correlates for magnetoencephalography: integration with magnetic resonance images. *Clin Phys Physiol Meas*, 12, Suppl. A:29–32, 1991.

[34] MS Hämäläinen, R Hari, RJ Ilmoniemi, J Knuutila, and OV Lounasmaa. Magnetoencephalography — theory, instrumentation, and applications to noninvasive studies of the working human brain. *Rev Mod Phys*, 65:413–497, 1993.

[35] MS Hämäläinen and RJ Ilmoniemi. Interpreting measured magnetic fields of the brain: estimates of current distributions. *Report*, TKK-F-A559, 1984.

[36] MS Hämäläinen and RJ Ilmoniemi. Interpreting magnetic fields of the brain: Minimum norm estimates. *Med Biol Eng Comp*, 32:35–42, 1994.

[37] MS Hämäläinen and J Sarvas. Feasibility of the homogeneous head model in the interpretation of neuromagnetic fields. *Phys Med Biol*, 32:91–97, 1987.

[38] MS Hämäläinen and J Sarvas. Realistic conductivity model of the human head for interpretation of neuromagnetic data. *IEEE Trans Biomed Eng*, 86:165–171, 1989.

[39] MA Howard, IO Volkov, PJ Abbas, H Damasio, MC Ollendieck, and MA Granner. A cronic microelectrode investigation of the tonotopic organization of human auditory cortex. *Brain Res*, 724:260–264, 1996.

[40] K Hugdahl and CG Brobeck. Hemispheric asymmetry and human electrodermal conditioning: the dichotic extinction paradigm. *Psychophys*, 23:491–499, 1986.

[41] RJ Ilmoniemi, MS Hämäläinen, and J Knuutila. The forward and inverse problems in the spherical model. In H Weinberg, G Stroink, and T Katila, editors, *Biomagnetism: Applications and theory*, pages 278–282. Pergamon, New York, 1985.

[42] NM Kane, SH Curry, SR Butler, and BH Cummins. Electrophysiological indicator of awakening from coma. *Lancet*, 341:688, 1993.

[43] E Kaukoranta, M Hämäläinen, J Sarvas, and R Hari. Mixed sensory nerve stimulations activate different cytoarchitectonic areas at the human primary somatosensory cortes SI. Neuromagnetic recordingsand statistical considerations. *Exp Brain Res*, 283:523–537, 1978.

[44] VO Kelhä, JM Pukki, RS Peltonen, AJ Penttinen, RJ Ilmoniemi, and JJ Heino. Design, construction, and performance of a large-volume magnetic shield. *IEEE Trans Mag*, MAG-18:260–270, 1982.

[45] N Kraus, T McGee, T Carrell, A Sharma, D Koch, C King, K Tremblay, and T Nicol. Neurophysiologic bases of speech discrimination. *Ear Hear*, 16:19–37, 1995.

[46] SW Kuffler, JG Nicholls, and AR Martin. *From neuron to brain. 2nd edition.* Sinauer Associates, Sunderland, 1984.

[47] T Kujala, K Alho, P Paavilainen, H Summala, and R Näätänen. Neural plasticity in processing of sound location by the early blind: an event-related potential study. *Electroenceph clin Neurophys*, 84:469–472, 1992.

[48] JL Lauter, P Herscovitch, C Formby, and ME Raichle. Tonotopic organization in human auditory cortex revealed by positron emission tomography. *Hear Res*, 8:190–205, 1985.

[49] C Liegois-Chauvel, A Musolino, J M Badier, P Marquis, and P Chauvel. Evoked potentials recorded from the auditory cortex in man: evaluation and topography of the middle latency components. *Electroenceph clin Neurophys*, 92:204–214, 1994.

[50] JP Mäkelä, M Hämäläinen, R Hari, and L McEvoy. Whole-head mapping of middle-latency auditory evoked magnetic fields. *Electroenceph clin Neurophys*, 92:414–421, 1994.

[51] JK Moore and KK Osen. The cochlear nuclei in man. *Am J Anat*, 154:393–418, 1979.

[52] FE Musiek. Neuroanatomy, neurophysiology, and central auditory assessment. Part II. The cerebrum. *Ear Hear*, 7:283–294, 1986.

[53] R Näätänen. *Attention and brain function.* N J Erlbaum, Hillsdale, 1992.

[54] R Näätänen, RJ Ilmoniemi, and K Alho. Magnetoencephalography in studies of human cognitive brain function. *Trends Neurosci*, 17:389–395, 1994.

[55] R Näätänen, P Paavilainen, H Tiitinen, D Jiang, and K Alho. Attention and mismach negativity. *Psychophys*, 30:436–450, 1993.

[56] R Näätänen and T Picton. The N1 wave of the human electric and magnetic response to sound: a review and an analysis of the component structure. *Psychophys*, 24:375–425, 1987.

[57] R Näätänen. Selective attention and stimulus processing: reflections in event-related potentials, magnetoencephalogram, and regional cerebral blood flow. In MI Posner and OSM Marin, editors, *Attention and performance XI*, pages 355–373. Erlbaum, Hillsdale, NJ, 1985.

[58] R Näätänen and AWK Gaillard. The N2 deflection of ERP and the orienting reflex. In AWK Gaillard and W Ritter, editors, *EEG correlates of information processing: Theoretical issues*, pages 119–141. North Holland, Amsterdam, 1983.

[59] R Näätänen and PT Michie. Early selective attention effects on the evoked potential. A critical review and reinterpretation. *Biol Psychol*, 8:81–136, 1979.

[60] R Näätänen, M Simpson, and NE Loveless. Stimulus deviance and evoked potentials. *Biol Psychol*, 14:53–98, 1982.

[61] JET Knuutila nad AI Ahonen, MS Hämäläinen, MJ Kajola, PO Laine, OV Lounasmaa, LT Parkkonen, JTA Simola, and CD Tesche. A 122-channel whole cortex SQUID system for measuring the brain's magnetic fields. *IEEE Trans Mag*, MAG-18:260–270, 1994.

[62] JB Nadol. Serial section reconstruction of the neural poles of hair cells in the human organ of Corti. II Outer hair cells. *Laryngosc*, 93:780–791, 1983.

[63] JB Nadol. Serial section reconstruction of the neural poles of hair cells in the human organ of Corti. I Inner hair cells. *Laryngosc*, 93:599–614, 1983.

[64] U Neisser. *Cognitive psychology.* Appleton-Century-Crofts, New York, 1967.

[65] J Numminen and RJ Ilmoniemi. Regularization of ill-conditioned linear systems: Application to biomagnetism. *Proc 26th Annu Conf Finn Phys Soc*, Tech Rep TKK-F-A697, Helsinki University of Technology, Espoo, Finland:17:11, 1992.

[66] PL Nunez. *Electric fields of the brain: The neurophysics of EEG.* Oxford University Press, New York, 1981.

[67] PL Nunez. *Neocortical dynamics and human EEG rhythms.* Oxford University Press, New York, 1995.

[68] D Oertel, SH Wu, and JA Hirsch. Electrical characteristics of cells and neuronal circuitry in the cochlear nuclei studied with intracellular recordings from brain slices. In GM Edelman, WE Gall, and WM Cowan, editors, *Auditory Function: Neurobiological bases of hearing*, pages 313–336. Wiley, New York, 1989.

[69] WW Orrison, JD Lewine, JA Sanders, and MF Hartshorne. *Functional Brain Imaging.* St. Louis: Mosby Year Book Inc., 1995.

[70] M Paavola, R Ilmoniemi, and L Sohlström. High performance magnetically shielded room for clinical measurements. In *Biomag96 Book of Abstracts.* 1997, in press.

[71] C Pantev, M Hoke, K Lehnertz, and B Lütkenhöner. Neuromagnetic evidence of an ampliotopic organization of the human auditory cortex. *Electroenceph clin Neurophys*, 72:255–231, 1989.

[72] C Pantev, M Hoke, K Lehnertz, B Lütkenhöner, G Anogianakis, and W Wittkowski. Tonotopic organization of the human auditory cortex revealed by transient auditory evoked magnetic fields. *Electroenceph clin Neurophys*, 69:160–170, 1988.

[73] R Parasunaman and J Beatty. Brain events underlying detection and recognition of weak sensory signal. *Science*, 210:80–83, 1980.

[74] RD Pasqual-Marqui, CM Michel, and D Lehman. Low resolution electromagnetic tomography: a new method for localizing electical activity in the brain. *Int J Psychophys*, 18(1):49–65, 1994.

[75] E Pekkonen, V Jousmäki, M Könönen, K Reinikainen, and J Partanen. Auditory sensory memory impairment on alzheimer's disease: An event-related potential study. *NeuroReport*, 5:2537–2540, 1994.

[76] E Pekkonen, M Huoti lai nen, J Vir ta nen, J Sinkkonen, T Rinne, RJ Ilmoniemi, and R Näätänen. Age-related functional differences between auditory cortices: a whole-head MEG study. *NeuroReport*, 6:1803–1806, 1995.

[77] W Penfield and T Rasmussen. *The cerebral cortex of man.* Macmillan, New York, 1950.

[78] JO Pickles. An introduction to the physiology of hearing. *Plenum Press*, 1983.

[79] JO Pickles and DP Corey. Mechano-electrical transduction by hair cells. *Trends Neurosci*, 15, 7:254–259, 1992.

[80] TW Picton, OG Lins, and M Scherg. The recording and analysis of event-related potentials. In F Boller and J Grafman, editors, *Handbook of Neuropsychology, Vol. 10.* Amsterdam: Elsevier, 1995.

[81] TW Picton, RT Rodriguez, RD Linden, and AC Maiste. The neurophysiology of human hearing. *Human Communic Canada*, 9:127–136, 1985.

[82] CW Ponton and M Don. The mismatch negativity in cochlear implant users. *Ear Hear*, 16:131–146, 1995.

[83] WS Pritchard. Psychophysiology of P300. *Psychol Bull*, 89:506–540, 1981.

[84] M Reite, P Teale, J Zimmerman, K Davis, and J Whalen. Source location of a 50 msec latency auditory evoked field component. *Electroenceph clin Neurophys*, 70:490–498, 1988.

[85] GL Romani, SJ Williamson, and L Kaufman. Tonotopic organization of the human auditory cortex. *Science*, 216:1339–1340, 1982.

[86] M Sams, P Paavilainen, K Alho, and R Näätänen. Auditory frequency discrimination and event-related potentials. *Electroenceph clin Neurophys*, 62:437–448, 1985.

[87] J Sarvas. Basic mathematics and electromagnetic concepts of the biomagnetic inverse problem. *Phys Med Biol*, 32:11–22, 1987.

[88] M Scherg. Fundamentals of dipole source potential analysis. In F Grandori, M Hoke, and G L Romani, editors, *Auditory evoked magnetic fields and electric potentials. Advances in Audiology*, volume 6, pages 40–69. Karger, Basel, 1990.

[89] E Schröger. Attentional capture and mismatch negativity. *Pshychophys*, 31:88–89, 1994.

[90] S Sutton, M Braren, J Zubin, and ER John. Evoked potential correlates of stimulus uncertainty. *Science*, 150:1187–1188, 1965.

[91] CD Tesche, MA Uusitalo, RJ Ilmoniemi, M Huotilainen, M Kajola, and O Salonen. Signal-space projection of MEG data characterize both distributed and well-localized neuronal sources. *Electroenceph clin Neurophys*, 95:189–200, 1995.

[92] LJ Trejo, DL Ryan-Jones, and AF Kramer. Attentional modulation of the mismatch negativity elicited by frequency differences between binaurally presented tone bursts. *Psychophys*, 32:319–328, 1996.

[93] MA Uusitalo and RJ Ilmoniemi. The signal-space projection (SSP) method for separating MEG or EEG into components. *Med Biol Eng Comp*, 1996, in press.

[94] HG Vaughan, Jr and W Ritter. The sources of auditory evoked responses recorded from the human scalp. *Electroenceph clin Neurophys*, 28:360–367, 1970.

[95] HG Vaughan, Jr, W Ritter, and R Simson. Topographic analysis of auditory event-related potentials. In HH Kornhuber and L Deecke, editors, *Motivation, motor and sensory processes of the brain: electrical potentials, behaviour and clinical use. Progress in brain research*, volume 54, pages 279–290. Elsevier, Amsterdam, 1980.

[96] C Verkindt, O Bertrand, F Perrin, JF Echallier, and J Pernier. Tonotopic organization of the human auditory cortex: N100 topography and multiple dipole model analysis. *Electroenceph clin Neurophys*, 96:143–156, 1995.

[97] JZ Wang, SJ Williamson, and L Kaufman. Kinetic images of neuronal activity of the human brain based on the spatio-temporal MNLS inverse: A theoretical study. *Brain Topog*, 7:193–200, 1995.

[98] WR Webster and LJ Garey. Auditory system. In G Paxinos, editor, *The human nervous system*, pages 889–944. Academic Press, New York, 1990.

[99] SF Witelson and DL Kigar. Sylvian fissure morphology and asymmetry in men and women: bilateral differences in relation to handedness in men. *J Comparat Neurol*, 323:326–340, 1992.

[100] MG Woldorff, CC Gallen, SA Hampson, SA Hillyard, C Pantev, D Sobel, and FE Bloom. Modulation of early sensory processing in human auditory cortex during auditory selective attention. *PNAS*, 90:8722–8726, 1993.

[101] MG Woldorff, SA Hackley, and SA Hillyard. The effects of channel-selective attention on the mismatch negativity wave elicited by deviant tones. *Psychophys*, 28:30–42, 1991.

[102] MG Woldorff and SA Hillyard. Attentional influence on the mismatch negativity. Commentary. *Behav Brain Sci*, 13:261–262, 1990.

[103] DL Woods, CC Claywood, RT Knight, GV Simpson, and M Naeser. Generators of middle- and long-latency auditory evoked potentials: implications from studies of patients with bitemporal lesions. *Electroenceph clin Neurophys*, 68:132–148, 1987.

[104] T Yamamoto, S J Williamson, L Kaufman, C Nicholson, and R Llinàs. Magnetic localization of neuronal activity in the human brain. *Proc Natl Acad Sci*, 85:8735–8736, 1988.

[105] B Yvert, O Bertrand, JF Echallier, and J Pernier. Improved dipole localization using local mesh refinement of realistic head geometries: an eeg simulation study. *Electroenceph clin Neurophys*, 99:79–89, 1996.